Biomaterials Science

PAPER

Check for updates

In vivo soft tissue reinforcement with bacterial nanocellulose†

Irene Anton-Sales, ‡[a] Soledad Roig-Sanchez, ‡[a] Kamelia Traeger, [b] Christine Weis, *[b] Anna Laromaine, [a] Pau Turon [b] and Anna Roig *[a]

The use of surgical meshes to reinforce damaged internal soft tissues has been instrumental for successful hernia surgery; a highly prevalent condition affecting yearly more than 20 million patients worldwide. Intraperitoneal adhesions between meshes and viscera are one of the most threatening complications, often implying reoperation or side effects such as chronic pain and bowel perforation. Despite recent advances in the optimization of mesh porous structure, incorporation of anti-adherent coatings or new approaches in the mesh fixation systems, clinicians and manufacturers are still pursuing an optimal material to improve the clinical outcomes at a cost-effective ratio. Here, bacterial nanocellulose (BNC), a bio-based polymer, is evaluated as a soft tissue reinforcement material regarding mechanical properties and *in vivo* anti-adhesive performance. A double-layer BNC laminate proved sufficient to meet the standards of mechanical resistance for abdominal hernia reinforcement meshes. BNC-polypropylene (BNC-PP) composites incorporating a commercial mesh have also been prepared. The *in vivo* study of implanted BNC patches in a rabbit model demonstrated excellent anti-adherent characteristics of this natural nanofibrous polymer 21-days after implantation and the animals were asymptomatic after the surgery. BNC emerges as a novel and versatile hernioplasty biomaterial with outstanding mechanical and anti-adherent characteristics.

1. Introduction

Abdominal hernias occur when internal organs protrude through weakened zones of the abdominal cavity. To date, surgical intervention is the only effective approach to repair such a highly prevalent condition that yearly affects more than 20 million patients worldwide.[1] Instrumental for successful hernia surgery has been the use of surgical meshes (*i.e.* hernioplasty) to reinforce the damaged region. Those implants are predominantly manufactured from synthetic polymers, mainly polypropylene (PP), and aim at providing mechanical support to the herniated area. Implantation of a non-resorbable PP-mesh has become the standard procedure for hernia repair, however, complications related to mesh implantation such as seroma, adhesions, chronic severe pain and infections are driving constant innovation in the field.[2,3]

Adhesions developed between PP-mesh and viscera, as a result of tissue reaction due to foreign body implant, are particularly threatening since they often cause complicated re-operations in the previously implanted area, increasing the surgical risk and the chances of suffering side effects such as chronic pain and bowel perforation.[4] High rates of adhesion are reported in approx. 15% of the cases one year after surgery, resulting in a high burden to healthcare systems.[5] Aiming to reduce the complications caused by those intraperitoneal adhesions, research efforts have been focused on improving the characteristics of PP meshes. Strategies include the optimization of mesh porous structure,[6] incorporation of anti-adherent coatings and improvements of mesh fixation systems (*i.e.* glueing).[7,8] Besides, multi-component grafts have been advocated as a well-suited strategy to isolate the PP mesh from the viscera by adding an additional layer of a synthetic[9,10] or natural biomaterial[11,12] that acts as an anti-adherent barrier. Despite recent advances, clinicians and manufacturers are still pursuing an optimal mesh to improve the clinical outcome and the cost-effectiveness ratio of hernioplasty procedures by leveraging the selection of materials, porous structure, mechanical resistance, anti-adhesive properties, biocompatibility, long term mechanical stability, tissue integration and conformability.[13]

Considering the requirements of hernia repair implants, the bio-based polymer bacterial nanocellulose (BNC) could be

a Institute of Materials Science of Barcelona (ICMAB-CSIC), Campus UAB, 08193 Bellaterra, Catalonia, Spain. E-mail: anna.roig@csic.es
b Department of Research and Development, B. Braun Surgical, S.A.U., Carretera de Terrassa 121, Rubí, 08191 Barcelona, Spain. E-mail: christine.weis@bbraun.com
†Electronic supplementary information (ESI) available. See DOI: 10.1039/d1bm00025j
‡Authors with equal contribution

deemed as a strong candidate for the above-mentioned tissue reinforcement application.[14] BNC is biotechnologically produced as a highly pure, non-soluble nanocellulose fibrillary network entrapping a large amount of liquid and exhibiting excellent mechanical properties.[15–17] These attributes have enabled an ever-increasing number of bio-applications in wound dressing and drug delivery.[18–20] Moreover, BNC is emerging as a high-performing alternative to repair other defects where non-biodegradable implants are desirable, such as damage of the dura mater,[21] the eardrum[22] or as an anti-fibrotic agent for cardiac implants.[23] As for soft tissue reinforcement, a hybrid biomaterial combining BNC with PP-meshes and its *in vitro* low adhesion properties has recently been described.[24] Besides, Zharikov and co-workers compared the anti-adhesive behaviour of BNC with PP meshes revealing a lower occurrence of adhesion in BNC-implanted dogs together with the absence of infections.[25] For that study, wet native BNC pellicles were employed and no mechanical tests were carried out. In more recent work, Rauchfuß *et al.* tested two surgical methods to implant wet BNC into the abdominal wall of rats.[26] These authors observed adhesion formation when using BNC as an abdominal wall replacement together with a tissue reaction assessed to be of low clinical significance. Interestingly, this work provides mechanical testing of BNC after explantation showing variable values and calling for future work on the suitability of BNC for hernia repair in terms of mechanical properties. These studies, although preliminary, concur with the absence of major postoperative complications and emphasize the underexploited potential of BNC in herniology.

Our work aims at providing further insight into the prospects of BNC for hernia repair surgery. To expand on the mechanical suitability of BNC for soft tissue reinforcement, the mechanical performance of several types of BNC implants —dry and wet forms as well as single to triple-layered BNC constructs— are evaluated. Furthermore, an *in vivo* study based on a novel animal model (rabbit) and the implantation of dry BNC is presented to demonstrate the anti-adherent properties of BNC.

2. Materials and methods

2.1 Bacterial nanocellulose (BNC) production

BNC films were obtained as previously described in Roig-Sanchez S. *et al.*[27] In brief, *Komagataeibacter xylinus* (*K. xylinus*) strain (NCIMB 5346, from CECT, Spain) was inoculated on 6 mL of Hestrin-Schramm (HS) fresh medium and expanded for 7 days at 30 °C. HS medium was prepared as follows: 5 g peptone, 5 g yeast, 20 g dextrose (Conda Lab), 1.15 g citric acid and 6.8 g $Na_2HPO_4 \cdot 12H_2O$ (Sigma-Aldrich) per 1 L of Milli-Q (MQ) water. Then, 0.5 mL of the mixture was transferred to 4.5 mL of fresh HS medium and let to proliferate for another three days. Finally, bacteria were diluted to a proportion 1 : 14 inoculum : HS medium and 65 mL were cultivated for 6 days in 12 × 12 cm plates (Labbox polystyrene Petri

dishes) at 30 °C. The square BNC pellicles formed at the liquid-air interface of the wells were harvested and cleaned 10 minutes in a 50% ethanol-water solution, twice with boiling water for 20 min and twice with 0.1 M NaOH (Sigma-Aldrich) at 90 °C for 20 min. Lastly, the films were washed with MQ water until neutralization and sterilized by autoclave (121 °C, 20 min). To obtain the dry and flat BNC films used in the mechanical and *in vivo* tests, BNC hydrogels were placed between two Teflon papers at 60 °C and with a 2 kg weight on top for 12 h as previously described.[27] Systems with two and three BNC layers were prepared by drying size-matched BNC pellicles in close contact following the same procedure. To achieve a smooth interface between the BNC films, the superficial water was removed by blotting BNC with filter paper and air bubble formation was avoided by applying manual pressure. BNC-PP composites were prepared similarly by placing fragments of PP meshes (Optilene® Mesh Elastic and Optilene® Mesh LP both from B. Braun Surgical, S.A.U., Spain), knitted with different pore sizes, in between two wet BNC films. The size of the BNC layers was larger than the PP meshes to allow the self-adhesion between BNC films to occur during drying.

2.2 Scanning electron microscopy (SEM)

For the SEM characterization of the native wet BNC structure, BNC hydrogels were supercritically dried (SC). For that, the as-obtained BNC films were placed within filter paper sheets and were subjected to a water-to-ethanol solvent exchange process. After two transfers of 3 h in absolute ethanol, the films were moved to a fresh ethanol bath, kept overnight and the resulting alcogel was dried by SC drying. SC drying was performed on a 300 mL capacity autoclave filled with ethanol which was pressurized to 100 bar at room temperature. Liquid CO_2 was dispensed for 1.5 h with a flow of 1 kg h^{-1} to exchange the solvent. Then, the reactor was heated up to 45 °C to reach supercritical conditions and supercritical CO_2 was pumped for 1 h keeping the same flow rate. Finally, the vessel was slowly depressurized to avoid pore collapse and BNC aerogels were obtained. For the SEM analysis of dry films, BNC hydrogels were dried as described in section 2.1.

FEI Magellan 400L XHR SEM under a high vacuum, with an acceleration voltage of 2 kV, current of 0.10 nA and a working distance of 5 mm was used to study the morphology of SC dried and dry BNC. The material was fixed with adhesive carbon tape on top of aluminium SEM holders. Dry BNC was sputtered with 5 nm Pt. BNC fibre diameter was calculated as the mean of 100 measurements obtained using Image-J software.

Cross-section images of multi-layered constructs were obtained with FEI Quanta 650GEG-ESEM under low vacuum conditions, an acceleration voltage of 20 kV, an electron beam spot of 4–5 and a working distance of 10 mm. Samples were cut with a PTFE coated blade (Personna GEM single edge, 3-facet stainless steel, 0.23 mm) and placed on holders with a 90° tilt.

2.3 Mechanical studies

Each BNC sheet was cut in 20 × 50 mm pieces and the weight, size and thickness were measured with an Acculab Atilon ATL-244-1 analytical balance, Stanley Millesimal rule and Mitutoyo 543-250B micrometer respectively. Results were computed from five replicas. Surface weight was calculated as the ratio between weight and area. Wet BNC samples were deposited on a filter paper to remove the excess of water and measurements were performed when the material was still wet. The thickness of the films was measured in the middle of the specimens. For wet samples, the plunger of the micrometer was lifted and lowered three times and the thickness was obtained when the value was stable for more than 2 s during the third time.

Zwick Z2.5 dynamometer with a load cell of 2.5 kN was used for tensile experiments. The clamps were metallic with a pneumatic flat rubber part in contact with the sample. The test velocity was 100 mm min^{-1}, the pressure of the clamps was 6 bars and the distance between them was 20 mm. The preload applied was 0.05 N. Strain and resistance to tearing (F_{max}) values were acquired.

Multi-layered systems were immersed in a 0.9% NaCl solution for 5 min for rehydration before the tensile study. Excess of liquid was removed as described before and water uptake (H_2O_{up}) percentage was calculated as $(m_w - m_d)/m_d \times 100$, where m_w is the weight of the wet sample after hydration and m_d is the weight of the dry sample before hydration. Surface weight, calculated as the ratio between dry weight and area, and thickness were obtained before the rehydration.

2.4 In vivo study

A scheme of the steps to BNC implantation is depicted in Fig. 4A. This study was conducted by FREY-TOX GmbH (Herzberg, Germany), a DAkkS (national accreditation body of Germany) accredited laboratory according to EN ISO/IEC 17025 and European guidelines 93/42/EWG as well as 90/385/EWG.

2.4.1. BNC implant preparation. Dry BNC patches were cut to a size of 7 × 3 cm with scissors and sterilized by a routine ethylene oxide (EtOx) cycle from B. Braun Surgical S.A.U. to sterilise non-absorbable meshes. Sterility was confirmed by submerging the EtOx-treated BNC into liquid culture medium for 14 days without detecting the appearance of turbidity. The resistance of the biomaterial to the EtOx cycle was assessed by Fourier-Transform Infrared Spectroscopy (FTIR) (Fig. S1†).

2.4.2. In vivo model. The in vivo implantation study was performed in five female SPF albino rabbits of the stock New Zealand White (Envigo, 58″ Venray Netherlands). The animals had a bodyweight from 3.4 to 4.2 kg. An acclimatization period of at least 5 days was allowed. General anaesthesia was induced by intramuscular injection of 35–40 mg kg^{-1} ketamine and 5–6 mg kg^{-1} xylazine (Serumwerke Bernburg AG, Bernburg, Germany). This rabbit species was chosen because of its convenient body proportion and proved suitability for studying hernia repair materials including meshes.[28]

In the literature, it is described that most post-surgical adhesion formation takes place approximately until day 8 post-implantation.[29] Hence, the follow-up time was set at 21-days based on our previous work endorsing it as a sufficient period to observe mature adhesions in an advanced healing process as well as to infer the integration of the biomaterial within the abdominal wall.[30]

2.4.3 Surgical procedure. The operation field was shaved, disinfected and the abdomen was covered in a sterile manner. A median laparotomy was performed and the patches were carefully applied onto the left native abdominal wall between the peritoneum and the visceral organs, avoiding folding of the implants. Subsequently, the BNC patches were fixed by 6 suture stitches with polypropylene (Optilene, B. Braun Surgical, S.A.U., USP 3-0) sutures. The wound was closed with a continuous muscle suture and continuous intracutaneous sutures. The skin was glued with Histoacryl®, a cyanoacrylate-based tissue glue (B. Braun Surgical, S.A.U., Spain). After the follow-up time of 21 days, the rabbits were anaesthetized (Ketamine 40 mg per kg body weight and Xylazine 6 mg per kg body weight) and subsequently euthanized (T61 intravenously).

Once the animals were sacrificed, tissue integration and adhesion formation were macroscopically examined. During explantation, the application site, as well as the abdomen in toto, were macroscopically evaluated. Possibly occurring adhesions were evaluated after dissection regarding their area extension in relation (%) to the total abdominal wall area implanted (7 × 3 cm). Furthermore, adhesions were defined to the following categories following the Zühlke scores as follows:[31]

Score I: String adhesions that are easy to separate (blunt detachment).

Score II: Adhesions being partially vascularized causing blunt to sharp detachment.

Score III: Adhesions having distinct vascularization, with sharp detachment only.

Score IV: Tight adhesions requiring sharp detachment causing damage to the organs.

The tissue integration was judged descriptively: no integration; mild integration = slight pull for uplifting the patch from the abdominal wall; and distinct integration = distinct pull uplifting from the abdominal wall with visible adhesion and vascularization.

2.5. Histological analysis

The central area of the implant (size approximately 1 × 3 cm) was extirpated and fixed on 4% buffered formalin for histological examination. Tissue sections were cut with a microtome and processed following standard procedures.[32] Haematoxylin/eosin (HE) was used as a general staining for judgment of tissue integration.

2.6 Statistical analysis

Quantitative data were analysed with GraphPad Prism 8.0.2 software using ordinary one-way ANOVA followed by Tukey's multiple comparison test. Statistical significance was accepted

at 0.05 and data are represented as means ± standard deviation.

3. Results

3.1 Single layered BNC patches

Firstly, single-layer BNC patches intended for hernioplasty applications were produced and characterized in terms of their macroscopic features, thickness and mechanical properties. Fig. 1A displays the simultaneous production of seventy-two 12 × 12 cm-BNC films summing up >1 m² of the biomaterial as a venue to attain increased amounts of BNC at a laboratory level. After 6 days at 30 °C, continuous BNC pellicles formed at the surface of the liquid culture (Fig. 1B). Upon cleaning and removing organic residues, a change in colour (from yellowish to translucent white) was appreciated (Fig. 1C).

Macro and microstructure of BNC in wet and dry conditions are depicted in Fig. 1(C, D) and (E, F) respectively. Since the morphology of wet as-synthetized BNC samples could not be observed with enough resolution using SEM, a supercritical (SC) dried film was used as this drying method maintains with high-reliability the architecture of native samples.[33] As exposed in Fig. 1D, SC-dried BNC films are highly porous and composed of entangled cellulose nanofibers of 15 ± 5 nm in diameter. Upon drying at 60 °C, BNC films become more transparent and thinner while the fibres compact and the porosity decreases (see inset in Fig. 1F).

High tensile stress is a basic demand for a biomaterial proposed for soft tissue reinforcement applications. Tensile stress ≥ 16 N cm⁻¹ has been used as a benchmark for safe reinforcement of the abdominal wall.[34] Accordingly, tensile strength experiments were conducted to test the mechanical properties of BNC films using this value as a threshold. Fig. 2 shows the mean values obtained from five BNC samples in dry (pink) and wet (blue) conditions. Before mechanical characterization, the original BNC films (12 × 12 cm) were cut in 20 × 50 mm samples and their thickness and surface weight (weight per area) were measured in both wet and dry forms. The surface weight is approximately 60 times higher for wet films than for its dried counterparts (654 ± 153 g m⁻² wet film; 11 ± 1 g m⁻² dry film). Upon drying, 98% of the surface weight is lost as the water is removed, indicating that cellulose nanofibers account for only 2% of the wet BNC mass. These results are in agreement with the thickness measurement as BNC films experience a decrease in thickness of more than 96% when dehydrated (from 445 ± 91 μm wet film; to 16 ± 8 μm dry film). For the mechanical characterization, the 20 × 50 mm BNC pieces were clamped with metallic clips containing a pneumatic flat rubber part to prevent the sliding of the samples (see the image in Fig. 2). The resistance to tear (F_{max}) of wet BNC is approximately 60% than that of dry BNC (5 ± 1 N cm⁻¹ and 8 ± 3 N cm⁻¹ respectively). On the contrary, the maximum strain increases 12-fold in wet conditions (24 ± 2% in comparison to 2.1 ± 0.5% for dry BNC). These data indicate that our single-layer BNC films (neither in wet nor in the dry state) do not meet the minimum mechanical resistance requirements of 16 N cm⁻¹ to be used as a PP mesh substitute.
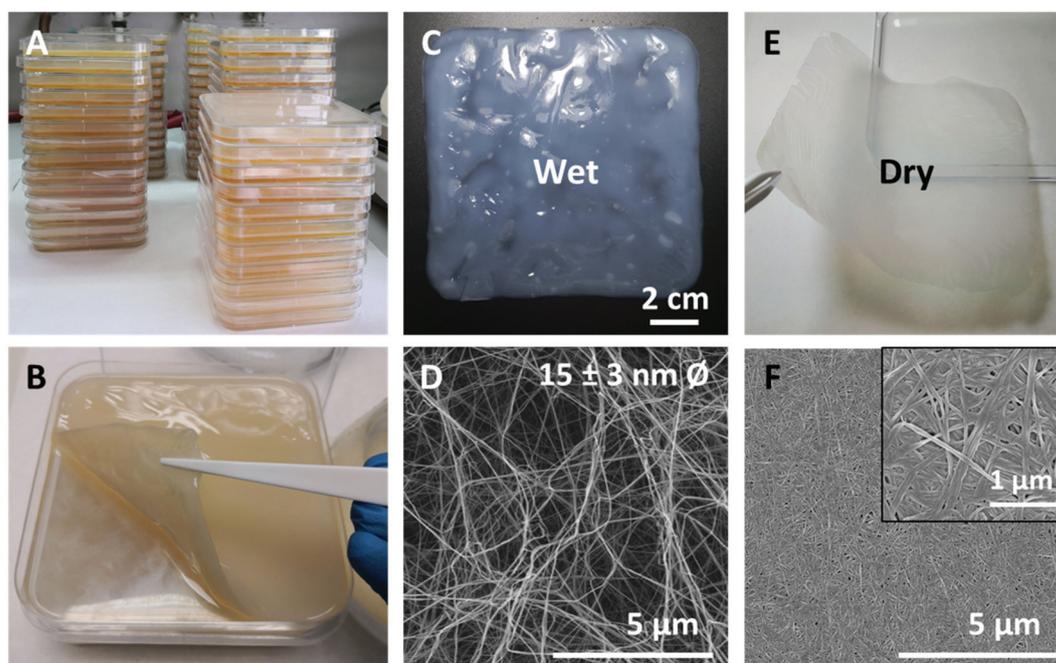
Fig. 1 BNC synthesis, wet and dry states and microstructure. (A) Numbering up BNC production at laboratory level. (B) A native wet BNC pellicle. (C) Wet form of BNC after cleaning and autoclaving. (D) SEM image of an SC dried BNC sample mimicking the microstructure of a wet BNC film. (E) Dry BNC film. (F) SEM image of the compact nanofiber conformation for dry BNC. Inset: higher magnification to better visualize the nanofibers arrangement.
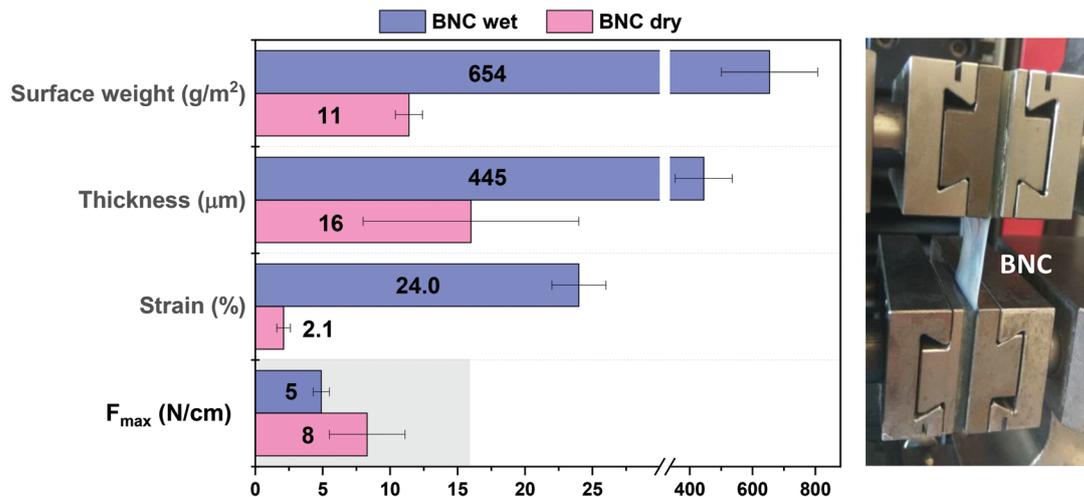
Fig. 2 Mechanical properties of single-layer BNC patches in wet and dry conditions and the experimental setup. Single-layered BNC implants did not meet the acceptance criteria of tensile stress resistance set at F_{max} = 16 N cm^{-1} (grey area). Statistically significant differences between dry and wet BNC samples were found for all the studied parameters except for the F_{max} (P-values < 0.001) (n = 5).

3.2 Laminated BNC patches and hybrids

To increase the mechanical resistance of the BNC patches, two strategies were followed: (i) preparation of multi-layered BNC meshes and (ii) combination of BNC with standard PP meshes. Our previous work showed that robust BNC stacks that endure hard manipulation even upon rehydration can be created by pilling up and drying together (*i.e.* applying weight) several wet BNC films. Upon drying, hydrogen bonding between the fibres of two films confers stability to the stack. The multilayers do not suffer delamination even when immersed in a liquid solution.[27] Accordingly, laminated patches were created by assembling 2 or 3 wet BNC films and subjected to the same mechanical characterization as the single BNC layers. Fig. 3A depicts the results of 2 and 3 layers of BNC (mean values of n = 5). All the obtained values were substantially higher than those of a single layer. As expected, thickness and surface weight increased as more layers were added. More precisely, thickness raised from 16 ± 8 μm (1 layer) to 23 ± 2 μm (2 layers) and 34 ± 6 μm (3 layers); and surface weight from 11 ± 1 g m^{-2} (1 layer) to 20 ± 1 g m^{-2} (2 layers) and 28 ± 2 g m^{-2} (3 layers). The multilayers were then rehydrated in a 0.9% NaCl solution for 5 min before performing mechanical studies to better simulate the physiological conditions. As shown in Fig. 3A, the laminate BNC presents a maximum strain of 14 ± 1 and 12 ± 3% and resistance to tearing of 26 ± 6 and 32 ± 9 N cm^{-1} for 2 and 3 layers respectively. For the double-layered BNC, the maximum strain increased almost 7-fold compared to a single BNC layer (dry form) while, the resistance to tear increased more than 3-fold. As expected, the triple-layer renders an even higher improvement in mechanical resistance (4-fold compared to a dry single layer). Note that the values of both the double and triple-layer laminates are above the set threshold of 16 N cm^{-1} for abdominal wall reinforcement applications. Improvements in mechanical properties (both the % of strain and the max force tolerated) of the stacked-BNC are statistically significant (P-values < 0.001) when compared to the BNC single-layer. Remarkably, during the tensile test, no peeling or separation of the layers was observed. This feature is also exemplified in Fig. 3B where a bi-layered sturdy BNC patch is shown. Both images —the macrostructure image and the cross-section SEM picture (inset)— illustrate the homogeneous adhesion between two BNC films. Moreover, the original transparency was maintained without macroscopic air bubbles trapped in the interface and the boundary area between the two BNC films could not be identified by SEM. Fig. S2† gathers the values obtained for the mechanical properties of all the studied systems for a clearer comparison.

Finally, BNC hybrid constructs incorporating commercial PP meshes were considered. Fig. 3C shows frontal and lateral pictures of a preliminary prototype of a sandwich-like multi-layer composite. The construct was prepared by taking advantage of the above-mentioned self-adhesion property of BNC. Note that the BNC-PP composite firmly incorporates PP meshes with different pore sizes. The thickness of the dry composites varied depending on the incorporated PP material between the BNC layers. That is, for a PP mesh with small pores (named SP-PP) a thickness of 332 ± 8 μm was obtained, while when a PP mesh with bigger pores was employed (BP-PP) thickness increased up to 589 ± 23 μm. An SEM cross-section study (Fig. 3D) showed good integration of the BP-PP mesh in between the BNC layers. Although the synthetic material did not adhere to the BNC layers, it was immobilized in an envelop-like structure due to the BNC self-adhesion in the contact areas in between the pores of the PP mesh and at the composite's contour (inset Fig. 3D). The stability of the hybrid structure was tested by rehydration in water. After 5 days, the moist envelope-like structure was flexible and easily handled without noticeable delamination as depicted in Fig. S3.†
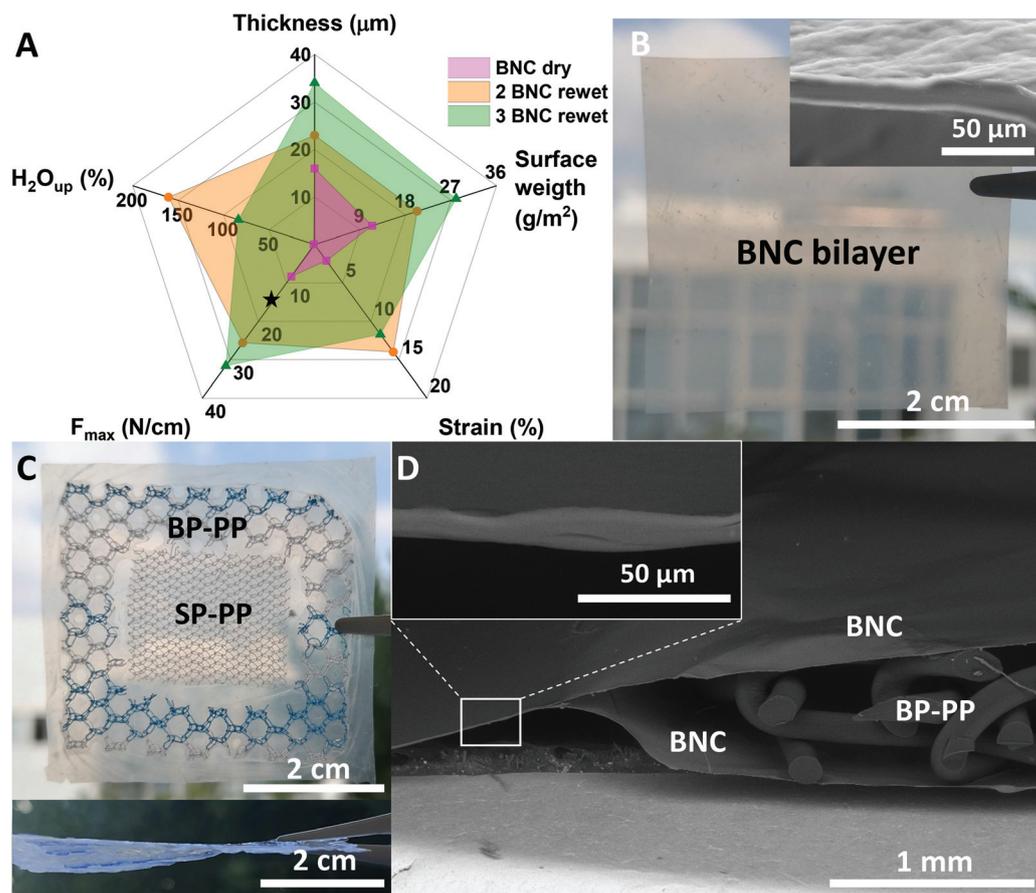
Fig. 3 Composite alternatives to increase the mechanical resistance of BNC-based implants. (A) Mechanical study of BNC multilayers comprised of 2 or 3 films. (n = 5) ★ indicates the resistance to tear threshold for tissue reinforcement materials (16 N cm^{-1}). (B) Picture of a BNC multilayer formed by 2 dry BNC films. Inset: SEM cross-section image where the interface between the two BNC layers is undetectable. (C) Preliminary BNC bilayer combination with PP meshes with different pore sizes. Upper panel: frontal view. Lower panel: a lateral image of the BNC-PP mesh composite. (D) SEM cross-section image of the BNC-PP composite. Inset: higher magnification of the cross-section to appreciate the continuous adhesion between BCN layers.

3.3 *In vivo* studies

Besides mechanical validation, a key characteristic required from soft tissue repair materials is their proficiency in minimizing adhesion-related complications and integration by surrounding tissues. Therefore, the next step was to assess the anti-adhesion properties of BNC with an *in vivo* rabbit model following the implantation process shown in Fig. 4A.

3.3.1 Macroscopic evaluation. Dry and sterile single layer BNC patches of 3 × 7 cm were selected for the *in vivo* study as being the ones with weaker mechanical characteristics and imposing the most stringent conditions. Single-layer BNC patches could be easily handled under operation-room settings, fold-free placing was readily achieved and fixation by suture was performed without complications (Fig. 4B). The semi-transparency of BNC was also convenient to avoid unintentional puncturing of blood vessels while suturing. During the application of the BNC patch, careful handling was necessary, nonetheless, the BNC patch allowed the secure application on the abdominal wall; no fracturing of the suture puncture

holes was observed and the BNC patches were removable with instruments and repositioned if needed. During the postoperative phase, all animals presented swift recovery. Analgesic treatment was only administered in the first postoperative days and a slight body weight gain was detected.

After the implantation period of 21 days, tissue integration was evaluated using observational criteria during the autopsy. The BNC patches displayed a general good integration to the abdominal wall whereas only marginal areas were not integrated. Adhesion level was examined and scored macroscopically considering prevalence (quantity) and type (quality) of the detected adhesions among BNC implants and the internal organs. In 4/5 animals adhesions were detected involving approximately 8% of the overall BNC surface. Although some fibrin accumulation and distinct vascularization were observed in all animals, only one rabbit presented a significant adhesion area (20%) as depicted in Fig. 4D. Three animals presented adhesions to the greater omentum and one animal to the cecum. Notably, one animal was completely free of adhesions (Fig. 4C). The implanted BNC patches were dominated
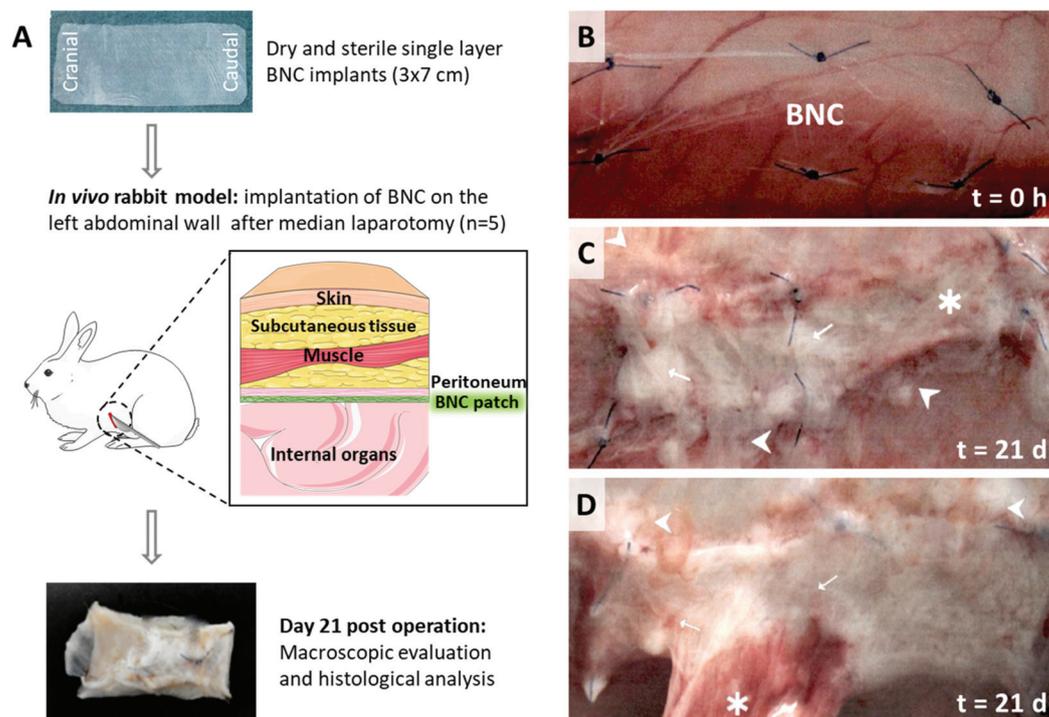
Fig. 4 Experimental design, macroscopic evaluation and adhesion assessment for two of the five animals studied. (A) Sketch showing the prepared BNC implant, the employed *in vivo* model and the evaluations performed. (B) Time 0: BNC patches were applied onto the left abdominal wall and fixed with six suture stitches (C) A2 explanted analysis after 21 days (best case scenario). → indicates fibrin accumulation, ▶ adjacent abdominal wall without adhesions and * marks vascularization. (D) A4 explanted analysis after 21 days (worst case scenario). → indicates vascularization, ▶ fibrin accumulations and * corresponds to adhesion.

by only one visible layer of fibrin. These macroscopic observations are gathered in Fig. S4† and Tables 1 and 2.

3.3.2. Histological evaluation. The central area of the implant (size ~1 × 3 cm) was extirpated and used for histological examinations. Representative HE-stained tissue sections from the five studied animals are shown in Fig. 5. The area surrounding the BNC patches presented a severe diffuse to granulomatous immune cell infiltration involving lymphocytes, heterophilic granulocytes, macrophages and solitary multinucleated giant cells. Also, a moderate active fibroplasia on the implanted zone was noted, as well as a good integration onto the abdominal wall and moderate neovascularization.

4. Discussion

We have investigated BNC patches for soft tissue reinforcement applications by dealing with two clinically relevant para-

Table 1 Individual adhesion observations. Results of the area free of adhesions, adhesion area, adhesion score and tissue integration for each studied animal

Animal number	6501	6507	6527	6564	6574
Code	A1	A2	A3	A4	A5
Area free of adhesions approx.	95%	100%	95%	80%	90%
Adhesion area approx.	5% to greater omentum	0%	5% to greater omentum	20% to greater omentum	10% to cecum
Adhesion score (Zühlke scores)	II – blunt to sharp detachment	No adhesions	II – blunt to sharp detachment	IV – sharp detachment	IV – sharp detachment
Tissue integration	Mild integration	Distinct integration	Distinct integration	Mild integration	Mild integration

Table 2 Overall adhesion observations. Summary of the macroscopic evaluation of adhesions between BNC implants and internal organs

No. of animals affected by adhesions	Area (%) free of adhesions	Adhesions area (%)	Organs involved in adhesion processes
4/5	92	8	Greater omentum (3 animals) Cecum (1 animal)
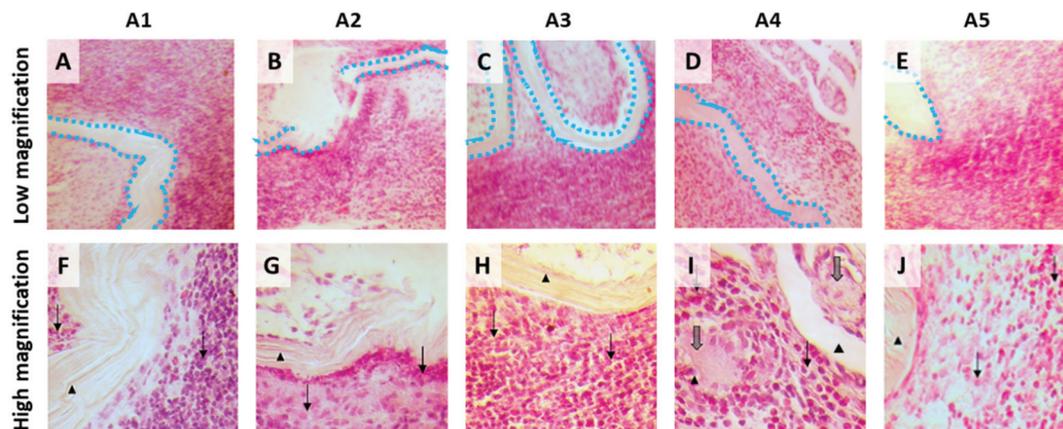
Fig. 5 HE-stained tissue sections of the BNC-implanted abdominal walls. A–E: Low magnification images of the five operated rabbits where the BNC implants have been highlighted with a blue dotted line to facilitate interpretation. For all cases, a good integration of the BNC patch together with an inflammatory reaction can be observed. F–J: Zoom-in to better appreciate the BNC implant (▶) and the presence of diverse inflammatory cells (lymphocytes, heterophilic granulocytes and macrophages) surrounding the implant (→). Solitary multinucleated giant cells were observed on A4 (I) (⇒).

meters; the mechanical resistance of constructs comprising one to three BNC layers and the *in vivo* anti-adherence properties of BNC. Before that, we characterized the BNC patches and present an increased BNC production (up to ~1 m^2) under laboratory settings to illustrate the feasibility of an up-scaled fabrication. However, to achieve an industrial manufacturing process, a more advanced system should be implemented such as the pilot-scale production processes reported by Kralisch *et al.*[35] and Beekmann *et al.*[36]

The mechanical characterization of as-synthesized BNC films (wet films) and after drying showed that wet BNC patches are thicker, more brittle but more stretchable than dry BNC patches. This confers to the wet-BNC a higher strain but, at the same time, makes the material less resistant to tear. After drying, the water content of BNC decreases drastically and the cellulose nanofibers condense, reducing their porosity[15] and their ability to rearrange upon tensile stress application. Thus, the dried form of BNC is stiffer and less stretchable than wet-BNC, making it more suitable for hernioplasty. Although the here studied single-layered BNC did not fulfil the mechanical resistance requirements to be used as a PP mesh substitute, thicker single layer BNC films grown for longer periods (>6 days) are expected to present sufficient mechanical support. We have previously reported that BNC fibres condense upon drying and form strong bonds among the cellulose nanofibers, this characteristic allowed us to arrange robust BNC multilayer laminates consisting of 2 or 3 layers.[24] The mechanical studies of those rehydrated BNC laminates have shown that the resistance to tear can be easily improved beyond the required 16 N cm^{-1} threshold for abdominal wall reinforcement applications. Even though previous studies confirmed the stability of BNC films in physiological conditions for up to 30 days,[37] the mechanical results of the laminates presented here were obtained after a 5 min-immersion in a saline solution and therefore, we cannot discard that the

mechanical properties of the films could be affected by longer hydration times.

Seeking to expand the library of BNC-based configurations for hernia repair patches, a composite patch integrating both BNC films and PP meshes was fabricated. This preliminary proof-of-concept demonstrates the possibility to, not only tune the mechanical properties of BNC but also to combine BNC films and PP meshes with different pore sizes. The sandwich-like BNC-PP structure was easy to prepare and exhibited robustness and good manageability both in dry and rehydrated conditions. This hybrid material shows the potential of BNC in the development of on-demand hybrid biomaterials for reinforcement of the abdominal wall but still requires further validation. The durability of the BNC-PP composites under physiological conditions is unknown at the moment and the need for additional strengthening of the composite (*i.e.* glueing with a cyanoacrylate-based biocompatible adhesive) could be considered in the future.[38]

We have recently validated BNC in diverse biological scenarios providing data on its cytocompatibility, lack of endotoxins (0.04 ± 0.01 Endotoxin Units per mL) after its biosynthesis as well as suturability and manageability in preclinical settings.[37,39] These findings, combined with the appealing mechanical properties reported here, positioned BNC as a suitable candidate for soft tissue repair patches and therefore *in vivo* studies were conducted. The anti-adhesion behaviour, biocompatibility and tissue integration characteristics of the BNC patches have been evaluated with a pilot animal study. BNC presented favourable surgical properties for this specific application in terms of suturability, manageability and accommodation to the implantation site. Moreover, the semi-transparent character of BNC was beneficial to avoid unintentional puncturing of underlying tissues. A general fold-free integration of the BCN material to the abdominal wall was detected in all the rabbits. Regarding adhesions between BNC

patches and internal organs, the overall area of the 5 implanted patches free of adhesions in this study is about 92%. Only a few adhesions were found after BNC implantation in the rabbit model, mostly involving the greater omentum which can be assessed as almost physiological since this organ is typically active in any post-surgical process. We hypothesize that the nanofibrillar microstructure of BNC, similar to that of the collagen networks on the extracellular matrix, favours the non-adherent characteristics of the BNC implants in accordance with the anti-fibrotic effect reported for cardiac implants wrapped with BNC.[20] The macroscopic evaluation showed that only a few adhesion strands were detected (overall at about 8% of the implant area) originated mainly on the suture stitches and at the border of the patches. For this pilot test, the BNC patches were fixed with sutures, even though sutures can cause foreign body responses and adhesions; indicating that suture-free administration methods could be worth exploring to diminish the adhesions even more. Overall, the macroscopic observation showed that good biocompatibility can be assumed for the BNC patches *in vivo* and the results indicate that BNC patches might act as a sufficient barrier to prevent adhesions in this rabbit sidewall model. Systemic tolerability of BNC can also be supposed from the good post-operative recovery of the test animals that occurred without notable complications.

On the histological analysis, all BNC implants appeared to be well integrated onto the abdominal wall, in good agreement with the macroscopic observations. An inflammatory response was observed at the *peri*-implanted area presenting fibroplasia and infiltration of diverse cell types (lymphocytes, heterophilic granulocytes, macrophages and solitary multinucleated giant cells) indicating a tissue reaction upon BNC. In a similar work, oxidized and laser-perforated BNC was employed in experimental surgery using a rabbit model.[40] One week after subcutaneous suture-free BNC implantation on the animal's back a positive integration of the BNC implants with the surrounding tissues was reported following our observations. Interestingly, Lai and co-workers stated a very low inflammatory response contrasting with the here presented histological analysis. Possibly, the distinct tissue responses arise from the different experimental protocols used (*i.e.* implantation site, use of sutures and longer implantation time, in our case) or the modifications of BNC. On the other hand, the previously cited work from Rauchfuß and colleagues[26] describes an inflammatory infiltration on the BNC patches judged to be of minimal clinical significance. We endorse that it could also apply to our *in vivo* study based on the witnessed lack of systemic toxicity. Besides, the good integration of the BNC implants –which were only indistinctly noticeable on the surrounding tissue– strengthens this reasoning. Nevertheless, the heterogeneous responses of the host immune system towards BNC implants indicate a need for future work.

Finally, the observation that a single layer of BNC could be sufficient to achieve low adhesions rates further emphasizes the attractiveness of BNC composites. Since a strong mechanical resistance is required for hernioplasty, composite BNC patches (either as multilayers or in combination with PP meshes) should be the mainstay of our future work.

5. Conclusions

In summary, BNC was investigated as a biomaterial for soft tissue reinforcement applications to tackle the long-lasting challenge of reducing adhesions between implants and internal organs after hernia surgery. While single-layer BNC does not present favourable mechanical properties, BNC laminates with 2 or 3 films are resistant enough to reach the minimal acceptance criteria for abdominal wall reinforcement applications. Notably, this simple stacking methodology supported the integration of commercial PP meshes between the BNC sheets opening future perspectives on BNC-PP hybrid biomaterials. Finally, an *in vivo* study revealed that BNC exhibits favourable surgical features in terms of suturability, manageability and accommodation to the implantation site. Besides, mild adhesion scores involving low percentages of the implant's area together with excellent integration capability on the *peri*-implant zone could be demonstrated. BNC elicited an inflammatory response that needs to be further investigated. Overall, our work proves that bio-based BNC possesses attractive mechanical and anti-adherent properties that could be valuable in the development of innovative hernia repair solutions.

Ethical statement

All animal procedures were performed according to Good Laboratory Guidelines and were carried out in accordance with the guidelines of EN ISO/IEC 17025 and European guidelines 93/42/EWG and 90/385/EWG as accredited by the national accreditation body of Germany (DAkkS, accreditation scope of records: D-PL-20600-01-00).

Author contributions

Irene Anton-Sales: conceptualization, methodology, validation, formal analysis, writing – original draft. Soledad Roig-Sanchez: conceptualization, methodology, validation, formal analysis, writing – original draft. Kamelia Traeger: methodology, validation, writing – review & editing. Christine Weis: conceptualization, resources, project administration, supervision, writing – review & editing. Anna Laromaine: conceptualization, funding acquisition, supervision, writing – review & editing. Pau Turon: conceptualization, resources, supervision, writing – review & editing. Anna Roig: conceptualization, project administration, funding acquisition, supervision, writing – review & editing.

Conflicts of interest

There are no conflicts to declare.

Acknowledgements

References

1 A. S. Kashyap, K. P. Anand and S. Kashyap, Inguinal and incisional hernias, *Lancet*, 2004, **363**(9402), 84.

2 R. Bittner, M. E. Arregui, T. Bisgaard, M. Dudai, G. S. Ferzli, R. J. Fitzgibbons, *et al.*, Guidelines for laparoscopic (TAPP) and endoscopic (TEP) treatment of inguinal hernia, *Surg. Endosc.*, 2011, **25**(9), 2773–2843.

3 F. Köckerling, R. Bittner, D. Adolf, R. Fortelny, H. Niebuhr, F. Mayer, *et al.*, Seroma following transabdominal preperitoneal patch plasty (TAPP): incidence, risk factors, and preventive measures, *Surg. Endosc.*, 2018, **32**(5), 2222–2231.

4 S. Muller, T. Langø, R. Brekken and B. Ystgaard, Degree of Adhesions After Repair of Incisional Hernia, *J. Soc. Laparoendosc. Surg.*, 2010, **14**, 399–404.

5 E. Chelala, Y. Debardemaeker, B. Elias, F. Charara, M. Dessily and J. L. Allé, Eighty-five redo surgeries after 733 laparoscopic treatments for ventral and incisional hernia: Adhesion and recurrence analysis, *Hernia*, 2010, **14**(2), 123–129.

6 M. Mirjavan and A. Asayesh, Asgharian Jeddi AA. The effect of fabric structure on the mechanical properties of warp knitted surgical mesh for hernia repair, *J. Mech. Behav. Biomed. Mater.*, 2017, **66**, 77–86.

7 C. Hollinsky, T. Kolbe, I. Walter, A. Joachim, S. Sandberg, T. Koch, *et al.*, Tensile strength and adhesion formation of mesh fixation systems used in laparoscopic incisional hernia repair, *Surg. Endosc.*, 2010, **24**(6), 1318–1324.

8 S. Lanzalaco, L. J. del Valle, P. Turon, C. Weis, F. Estrany, C. Alemán, *et al.*, Polypropylene mesh for hernia repair with controllable cell adhesion/de-adhesion properties, *J. Mater. Chem. B*, 2020, **8**(5), 1049–1059.

9 P. J. Emans, M. H. F. Schreinemacher, M. J. J. Gijbels, G. L. Beets, J. W. M. Greve, L. H. Koole, *et al.*, Polypropylene meshes to prevent abdominal herniation. Can stable coatings prevent adhesions in the long term?, *Ann. Biomed. Eng.*, 2009, **37**(2), 410–418.

10 S. Lanzalaco, P. Turon, C. Weis, C. Mata, E. Planas, C. Alemán, *et al.*, Toward the New Generation of Surgical Meshes with 4D Response: Soft, Dynamic, and Adaptable, *Adv. Funct. Mater.*, 2020, **2004145**, 1–9.

11 N. Udpa, S. R. Iyer, R. Rajoria, K. E. Breyer, H. Valentine, B. Singh, *et al.*, Effects of Chitosan Coatings on Polypropylene Mesh for Implantation in a Rat Abdominal Wall Model, *Tissue Eng., Part A*, 2013, **19**(23), 2713–2723.

12 F. Pomilio Di Loreto, A. Mangione, E. Palmisano, J. I. Cerda, M. J. Dominguez, G. Ponce, *et al.*, Dried human amniotic membrane as an antiadherent layer for intraperitoneal placing of polypropylene mesh in rats, *Surg. Endosc.*, 2013, **27**(4), 1435–1440.

13 F. Basile, A. Biondi and M. Donati, Surgical approach to abdominal wall defects: History and new trends, *Int. J. Surg.*, 2013, **11**(S1), S20–S23.

14 I. Anton-Sales, U. Beekmann, A. Laromaine, A. Roig and D. Kralisch, Opportunities of Bacterial Cellulose to Treat Epithelial Tissues, *Curr. Drug Targets*, 2019, **20**(8), 808–822.

15 M. Zeng, A. Laromaine and A. Roig, Bacterial cellulose films: influence of bacterial strain and drying route on film properties, *Cellulose*, 2014, **21**(6), 4455–4469.

16 S. Wang, F. Jiang, X. Xu, Y. Kuang, K. Fu, E. Hitz, *et al.*, Super-Strong, Super-Stiff Macrofibers with Aligned, Long Bacterial Cellulose Nanofibers, *Adv. Mater.*, 2017, **29**(35), 1702498.

17 S. Q. Chen, P. Lopez-Sanchez, D. Wang, D. Mikkelsen and M. J. Gidley, Mechanical properties of bacterial cellulose synthesised by diverse strains of the genus Komagataeibacter, *Food Hydrocolloids*, 2018, **81**, 87–95.

18 H. Ullah, F. Wahid, H. A. Santos and T. Khan, Advances in biomedical and pharmaceutical applications of functional bacterial cellulose-based nanocomposites, *Carbohydr. Polym.*, 2016, **150**, 330–352.

19 D. Klemm, E. D. Cranston, D. Fischer, M. Gama, S. A. Kedzior, D. Kralisch, *et al.*, Nanocellulose as a natural source for groundbreaking applications in materials science: Today's state, *Mater. Today*, 2018, **21**(7), 720–748.

20 L. Bacakova, J. Pajorova, M. Bacakova, A. Skogberg, P. Kallio, K. Kolarova, *et al.*, Versatile Application of Nanocellulose: From Industry to Skin Tissue Engineering and Wound Healing, *Nanomaterials*, 2019, **9**(2), 164.

21 F. M. Lima, F. C. M. Pinto, B. L. Andrade-da-Costa, J. G. Silva, O. Campos Júnior and J. L. Aguiar, Biocompatible bacterial cellulose membrane in dural defect repair of rat, *J. Mater. Sci.: Mater. Med.*, 2017, **28**(37).

22 F. C. A. Silveira, F.C. M. Pinto, S. Caldas Neto Sda, M. de C. Leal, J. Cesário and J. L. Aguiar, Treatment of tympanic membrane perforation using bacterial cellulose: a randomized controlled trial, *Braz. J. Otorhinolaryngol.*, 2016, **82**(2), 203–208.

23 F. Robotti, I. Sterner, S. Bottan, J. M. Monné Rodríguez, G. Pellegrini, T. Schmidt, *et al.*, Microengineered biosynthesized cellulose as anti-fibrotic in vivo protection for cardiac implantable electronic devices, *Biomaterials*, 2020, **229**, 119583.

24 K. Ludwicka, M. Kolodziejczyk, E. Gendaszewska-Darmach, M. Chrzanowski, M. Jedrzejczak-Krzepkowska, P. Rytczak,

et al., Stable composite of bacterial nanocellulose and perforated polypropylene mesh for biomedical applications, *J. Biomed. Mater. Res., Part B*, 2019, **107**(4), 978–987.

25 A. N. Zharikov, V. G. Lubyansky, E. K. Gladysheva, E. A. Skiba, V. Budaeva, E. N. Semyonova, *et al.*, Early morphological changes in tissues when replacing abdominal wall defects by bacterial nanocellulose in experimental trials, *J. Mater. Sci. Mater. Med.*, 2018, **29**(7).

26 F. Rauchfuß, J. Helble, J. Bruns, O. Dirsch, U. Dahmen, M. Ardelt, *et al.*, Biocellulose for incisional hernia repair—an experimental pilot study, *Nanomaterials*, 2019, **9**(2), 1–11.

27 S. Roig-Sanchez, E. Jungstedt, I. Anton-Sales, D. C. Malaspina, J. Faraudo, L. A. Berglund, *et al.*, Nanocellulose films with multiple functional nanoparticles in confined spatial distribution, *Nanoscale Horiz.*, 2019, **4**, 634–641.

28 J. C. Y. Chan, K. Burugapalli, Y. S. Huang, J. L. Kelly and A. Pandit, A clinically relevant in vivo model for the assessment of scaffold efficacy in abdominal wall reconstruction, *J. Tissue Eng.*, 2017, **8**, 1–11.

29 G. S. DiZerega and J. D. Campeau, Peritoneal repair and post-surgical adhesion formation, *Hum. Reprod. Update*, 2001, 7(6), 547–555.

30 R. A. Lang, P. M. Grüntzig, C. Weisgerber, C. Weis, E. K. Odermatt and M. H. Kirschner, Polyvinyl alcohol gel prevents abdominal adhesion formation in a rabbit model, *Fertil Steril*, 2007, **88**(4 suppl.), 1180–1186.

31 H. Kataria and V. P. Singh, Liquid Paraffin vs Hyaluronic Acid in Preventing Intraperitoneal Adhesions, *Indian J. Surg.*, 2017, **79**(6), 539–543.

32 J. F. Kukleta, C. Freytag and M. Weber, Efficiency and safety of mesh fixation in laparoscopic inguinal hernia repair using n-butyl cyanoacrylate: Long-term biocompatibility in over 1, 300 mesh fixations, *Hernia*, 2012, **16**(2), 153–162.

33 M. E. El-Naggar, S. I. Othman, A. A. Allam and O. M. Morsy, Synthesis, drying process and medical application of polysaccharide-based aerogels, *Int. J. Biol. Macromol.*, 2020, **145**, 1115–1128.

34 U. Klinge, B. Klosterhalfen, J. Conze, W. Limberg, B. Obolenski, A. P. Öttinger, *et al.*, Modified mesh for hernia repair that is adapted to the physiology of the abdominal wall, *Eur. J. Surg.*, 1998, **164**(12), 951–960.

35 D. Kralisch, N. Hessler, D. Klemm, R. Erdmann and W. Schmidt, White biotechnology for cellulose manufacturing–the HoLiR concept, *Biotechnol. Bioeng.*, 2010, **105**(4), 740–747.

36 U. Beekmann, L. Schmölz, S. Lorkowski, O. Werz, J. Thamm, D. Fischer, *et al.*, Process control and scale-up of modified bacterial cellulose production for tailor-made anti-inflammatory drug delivery systems, *Carbohydr. Polym.*, 2020, 116062.

37 I. Anton-Sales, J. C. D'Antin, J. Fernández-Engroba, V. Charoenrook, A. Laromaine, A. Roig, *et al.*, Bacterial nanocellulose as a corneal bandage material: A comparison with amniotic membrane, *Biomater. Sci.*, 2020, **8**(10), 2921–2930.

38 R. Jain and S. Wairkar, Recent developments and clinical applications of surgical glues: An overview, *Int. J. Biol. Macromol.*, 2019, **137**, 95–106.

39 I. Anton-Sales, S. Roig-Sanchez, M. J. Sánchez-Guisado, A. Laromaine and A. Roig, Bacterial nanocellulose and titania hybrids: cytocompatible and cryopreservable cell carriers, *ACS Biomater. Sci. Eng.*, 2020, **6**(9), 4893–4902.

40 C. Lai, K. S. Hu, Q. L. Wang, L. Y. Sheng, S. J. Zhang and Y. Zhang, Anti-Adhesion Mesh for Hernia Repair Based on Modified Bacterial Cellulose, *Starch/Staerke*, 2018, **70**(11–12), 1–10.